Patient-specific treatment planning of electrochemotherapy: Procedure design and possible pitfalls

Denis Pavliha [a], Bor Kos [a], Anže Županič [a], Marija Marčan [a], Gregor Serša [b], Damijan Miklavčič [a],*

[a] *University of Ljubljana, Faculty of Electrical Engineering, Tržaška 25, SI-1000 Ljubljana, Slovenia*
[b] *Institute of Oncology, Zaloška 2, SI-1000 Ljubljana, Slovenia*

ARTICLE INFO

ABSTRACT

Electrochemotherapy uses electroporation for enhancing chemotherapy. Electrochemotherapy can be performed using standard operating procedures with predefined electrode geometries, or using patient-specific treatment planning to predict electroporation. The latter relies on realistic computer models to provide optimal results (i.e. electric field distribution as well as electrodes' position and number) and is suitable for treatment of deep-seated tumors.

Since treatment planning for deep-seated tumors has been used in radiotherapy, we expose parallelisms with radiotherapy in order to establish the procedure for electrochemotherapy of deep-seated tumors. We partitioned electrochemotherapy in the following phases: the mathematical model of electroporation, treatment planning, set-up verification, treatment delivery and monitoring, and response assessment. We developed a conceptual treatment planning software that incorporates mathematical models of electroporation. Preprocessing and segmentation of the patient's medical images are performed, and a 3D model is constructed which allows placement of electrodes and implementation of the mathematical model of electroporation.

We demonstrated the feasibility of electrochemotherapy of deep-seated tumors treatment planning within a clinical study where treatment planning contributed to the effective electrochemotherapy treatment of deep-seated colorectal metastases in the liver. The described procedure can provide medical practitioners with information on using electrochemotherapy in the clinical setting. The main aims of this paper are: 1) to present the procedure for treating deep-seated tumors by electrochemotherapy based on patient-specific treatment planning, and 2) to identify gaps in knowledge and possible pitfalls of such procedure.

© 2012 Elsevier B.V. All rights reserved.

1. Introduction

When a cell is exposed to a sufficiently intense transient external electric field, the permeability of its membrane is increased [1]. This allows molecules that otherwise lack a membrane transport mechanism to enter the cell. Electroporation, as the phenomenon was named, can therefore be used to control the transport of different molecular species in and out of the cell and even induce controlled cell death if the parameters of the electric field are chosen appropriately [2].

Even though the exact molecular mechanisms of electroporation are not yet fully elucidated, it is being used in several medical applications, e.g. electrochemotherapy [3] (which is currently used in daily clinical practice for treatment of superficial tumor nodules in more than 80 clinical centers around Europe [4]), gene therapy [5],

and irreversible electroporation (for non-thermal ablation purposes) [6]. Electrochemotherapy combines cancer drugs, such as bleomycin or cisplatinum, with short high-voltage electric pulses, and achieves approximately 80% objective responses irrespective of the histological type of the tumor [7]. When planning electrochemotherapy, we can choose between two possible treatment planning modes: 1) following standard operating procedures with predefined geometry of electrodes based on models to predict electroporation, or 2) patient-specific treatment planning. Electrochemotherapy based on predefined geometries was described for skin tumors [7] and brain tumors [8,9] and several clinical trials are registered and are ongoing [10,11]. The first deep-seated tumors were treated and reported recently with electrochemotherapy and irreversible electroporation using long needle variable geometry electrodes, which clearly demonstrated that patient-specific treatment planning is needed [12–15].

Other electroporation-based therapies are also at the stage of clinical trials. Researchers have considerably increased the efficacy of electroporation-based gene transfer for gene therapy and DNA vaccination [16–19]. Furthermore, irreversible electroporation has been demonstrated in prostate, liver and brain *in vivo* on experimental animals [20] and in patients [21]. As a non-thermal ablation technique,

* Corresponding author. Tel.: +386 1 4768456; fax: +386 1 4264658.
E-mail addresses: denis.pavliha@fe.uni-lj.si (D. Pavliha), bor.kos@fe.uni-lj.si (B. Kos), anze.zupanic@fe.uni-lj.si (A. Županič), marija.marcan@fe.uni-lj.si (M. Marčan), gsersa@onko-i.si (G. Serša), damijan.miklavcic@fe.uni-lj.si (D. Miklavčič).

irreversible electroporation can be used to cause cell death while preserving extra-cellular tissue scaffolding [22], which greatly facilitates tissue healing after tissue ablation.

To bring the benefits of all these electroporation-based therapies to patients, treatment planning (predefined geometry-based or patient-specific) is necessary. By taking into account the patient's anatomy and numerically predicting the electroporation effects of the high-voltage electric pulses, optimal position of the electrodes can be determined, thereby assuring adequate electroporation of the tumor and limiting electroporation of the healthy tissue. We have taken radiotherapy treatment planning, that has been of paramount importance in the success of radiotherapy in the last 50 years, as the basis for the design of treatment planning in electrochemotherapy. We have already demonstrated in a proof-of-principle study [15] that anatomically realistic computer models of target tissue can be built based on medical imaging and by using finite element modeling for calculating the electric field distribution in the tissue, an efficient treatment plan can be prepared for treating deep-seated colorectal metastases in the liver. The main aims of this paper thus are: 1) to present procedures for deep-seated tumors electrochemotherapy based on patient-specific treatment planning, and 2) to identify gaps in knowledge and possible pitfalls of such procedures.

2. Background

Patient-specific treatment planning has been successfully introduced to and is widely used in radiotherapy, which like electroporation is also based on the interaction between a physical agent (radiation in radiotherapy, and electric field in electroporation) and biological tissue [23]. Radiotherapy is a cancer-treatment procedure where energy is deposited locally into the patient's body by a targeted radiation beam. The damage caused by the beam is not tumor-specific; the maximum allowed radiation dose to the tumor is thus limited by the dose the healthy tissue along the radiation path can withstand [24]. The main goal of radiotherapy is to cause enough radiation damage so that tumor cells get permanently inhibited and their growth can be delayed infinitively; therefore, tumor cells cannot proliferate further.

Radiotherapy consists of the following steps: simulation, treatment planning, set-up verification, beam delivery, and response assessment [23], as described in Table 1. Simulation is based on the patient's anatomy; the patient is scanned in order to obtain medical images (using e.g. Computed Tomography – CT or Magnetic Resonance Imaging – MRI) in the same position as expected to be when exposed to the radiation beam. Treatment planning starts by using the acquired medical images for generating a three-dimensional model. First, the target volumes are defined by the radiologist based on the image data in order to calculate the appropriate radiation dose, then the treatment plan is developed by numerical modeling and optimization – mathematical models of radiation damage in biological tissues have been developed in the first half of the 20th century and are, with some adjustments, still used today [25]. After the calculations, the plan is transferred to the controller device that manages the functioning of the irradiating device (e.g. a linear accelerator) that delivers the radiation beam. The set-up verification consists of examining the patient's position (e.g. using laser-based detectors) in order to coincide with the scanned medical images, and to reflect consequently the dose data from the generated treatment plan. Finally, beam delivery is executed and response assessment is performed later on by obtaining a new set of medical images and validating the treatment.

For the purposes of establishing procedures for deep seated tumors electrochemotherapy based on patient-specific treatment planning, we can expose parallels between electrochemotherapy and radiotherapy, as already suggested [8]. In radiotherapy, the radiation dose has to be high enough in the tumor volume to kill all the tumor cells, whereas in electrochemotherapy, the electric field in the tumor volume needs to be sufficiently strong, and the exposure long enough, to cause cell membrane electroporation [12]. Similarly to radiotherapy, electrochemotherapy of deep-seated tumors can also be partitioned into several steps: mathematical model of electroporation, treatment planning, set-up verification, treatment, and response assessment (Table 1). Therefore, in establishing procedure for electrochemotherapy of deep-seated tumors based on patient-specific treatment planning, radiotherapy treatment planning can serve as a well-established example.

The first step of designing electrochemotherapy of deep-seated tumors is to create a suitable numerical model of electroporation, at both cellular and tissue levels by determining material properties (electrical conductivity) as well as electroporation mechanisms that are related to the electric field distribution [26]. After patient-specific data are transferred to the model it can be used in the treatment planning procedure. The treatment planning consists of several phases: image import, image pre-processing, segmentation, three-dimensional model generation, electrode placement, implementation of the mathematical model of electroporation, and optimization of the results: the electric field distribution as well as the number of electrodes and electrodes' positions. The position of electrodes needs to be verified intraoperatively as part of the set-up verification in order to assure the treatment plan is accurately followed. Postoperative response assessment is required approximately 4–8 weeks after the treatment in order to determine effectiveness of electrochemotherapy by radiological imaging or tumor histology: if the patient is rescheduled for reoperation (as part of a two stage procedure [27]) the metastasis is resected and also histologically evaluated.

Table 1
Parallelism and similarities between radiotherapy and electrochemotherapy of deep-seated tumors.

Radiotherapy	Electrochemotherapy of deep-seated tumors
Simulation – medical imaging (CT or a combination of CT with MR or PET) of the patient	Mathematical model of electroporation: cell- and tissue-level models of electroporation.
Treatment planning: delineation of target volumes, definition of dose constraints, construction of the mathematical model geometry, calculation of a suitable plan by numerical modeling and optimization – number of fractions, position and intensity of the beams	Treatment planning: medical imaging (CT or MR, possible combination with PET) of the patient, delineation of target volumes, construction of the mathematical model geometry, calculation of a suitable plan by numerical modeling and optimization – number and positions of electrodes used, intensity of the used electric pulses
Set-up verification: medical imaging (CT or MRI) is used for verifying the position of the patient and target tissues, in subsequent session lasers and tattoo marks are used together with ultrasound (US) and other imaging modalities	Set-up verification: optimal electrode positions are registered on the original medical images; electrode positions are verified using intraoperative ultrasound (US)
Treatment delivery and monitoring: radiation is delivered according to the treatment plan, while imaging is used to control for breathing movements	Treatment delivery and monitoring: after electrode insertion and chemotherapeutic injection, electric pulses are delivered, current and voltage are measured to control for possible errors during electric pulse delivery
Response assessment: post-treatment measurement of tumor size or biological tumor markers with medical imaging	Response assessment: post-treatment measurement of tumor size or biological tumor markers with medical imaging and/or histology, compared to pre-treatment medical images.

3. Methodology

3.1. Mathematical model of electroporation

Mathematical modeling on the level of tissues and considering bulk tissue properties has been used in the field of tissue electroporation for more than a decade [28,29]. Initially, the models were focused on determining electric field distribution for different electrode geometries and analyzing the importance of the distribution for the effectiveness of electrochemotherapy. In subsequent studies, a correlation between the strength of the electric field, coverage of the tumor and electrochemotherapy effectiveness was established [30]. Electric field thresholds for reversible and irreversible electroporation were determined for various tissues, including liver [31] and muscle [32] by comparing tissue changes and histology with electric field calculation in geometrically correct models. It needs to be emphasized, however, that threshold values of electric field at which cell membrane electroporation occurs were determined for specific pulse parameters, i.e. most of the time for 8 pulses of 100 μs duration delivered at 1 Hz pulse repetition frequency. However, the electric field amplitude at which membrane permeabilization occurs depends on the pulse parameters (the number and the length of the pulses). Later, electroporation effects on tissue conductivity were incorporated in the mathematical models [33,26,31] which were validated by comparing the predicted and the measured electric currents during electric pulse delivery [33]. Electroporation thresholds (8×100 μs pulses) for liver tissue were determined to be 460 V/cm and 700 V/cm for reversible and irreversible electroporation, respectively [26,31]. In addition to electric field threshold values, which depend greatly on the pulse duration and the number of pulses delivered [34,2,35] but also on the method of detection [36] it has not been yet established how fast and how much the tissue conductivity increases during electroporation [33]. Currently, it is being estimated that during electroporation, the conductivity increases by a factor of 3–4, which yields good agreement between calculated and measured current values. The increase of conductivity was stipulated to correlate with the occurrence of electroporation, which was later demonstrated also in dense cell suspension experiments [37] and in vivo [38]. The values of the electric field for irreversible electroporation were later demonstrated to be most probably higher than originally reported [39], but have not yet been equivocally determined.

3.2. Treatment planning software

We developed a proof-of-concept principle computer software in order to fully devise and elaborate treatment planning for electrochemotherapy. The proof-of-concept electrochemotherapy treatment planning software was developed as a Windows (Microsoft, Redmond, USA, 1985–2011) application; the software was constructed in the Microsoft C# programming language within the Microsoft .NET Framework v3.5 (Microsoft, Redmond, USA, 2007) using Microsoft Visual Studio 2008 integrated development environment (Microsoft, Redmond, USA, 2007).

3.2.1. Image import

To generate representative models that can be used as input data for patient-specific electrochemotherapy treatment planning, scanned medical images (e.g. CT or MRI) of the patient are required. A currently commonly used standard for medical imaging is Digital Imaging and Communication in Medicine (DICOM) [40]. DICOM is used as the standard for encapsulating medical images that are obtained from e.g. CT or MRI scanners. Therefore, DICOM images are read and imported into the electrochemotherapy treatment planning software as input data.

Moreover, a conversion of DICOM images is required to allow further image processing. Namely, upon import of the medical images into the electrochemotherapy treatment planning software, the images are deposited into the working storage memory (e.g. memory streams that are located in the Random Access Memory – RAM). If we want to access them as raw data the images need to be converted into such a format; therefore, a conversion from DICOM into some other format, preferably uncompressed raw 8-bit data, is required. In case of the 8-bit format, 8 bits describe a single pixel intensity and a short header is also present to describe the dimensions of the medical images.

At this stage of development, a manual conversion from DICOM to bitmap data using commercially available computer graphics software Adobe Photoshop CS4 (Adobe Systems Inc., San Jose, CA, USA, 2008) is performed. Manual conversion is performed mainly because DICOM is a complex standard and a suitable implementation would require extensive development which has not been possible yet. Nevertheless, bitmap data can be interpreted by our software without problems due to native bitmap implementation in the Microsoft .NET Framework v3.5 (Microsoft, Redmond, USA, 2007). Then, the bitmap data is converted into raw 8-bit data within the electrochemotherapy treatment planning software.

3.2.2. Image pre-processing

Image pre-processing is required to prepare the medical (e.g. CT or MRI) images for image segmentation. Since the segmentation is based on feature extraction, the images are first transformed by means of pre-processing procedures in order to minimize bias of intensities [41]. Because medical images for electrochemotherapy planning purposes may steam from sources with different modalities (e.g. CT or MRI), a single set of pre-processing procedures cannot be implemented; a parameterized pre-processing software module with possibility of dynamically allocating pre-processing procedures is incorporated into the treatment planning software instead.

Pre-processing begins with the analysis of the images; analysis is used to determine the main intensity components that are present in the images, which allows implementation of intensity-based pre-processing procedures, i.e. threshold-based algorithms [42]. Such an analysis begins by showing the electrochemotherapy treatment planning software user (i.e. the attending physician) a histogram of all the intensities that are represented in the medical images' collection. An example of such a histogram is shown in Fig. 1 where relative intensities' representation (ordinate) is presented as a function of the 8-bit intensity range (abscissa).

As seen in Fig. 1, five thresholds delimit six main intensity components: one at the beginning, four in the middle, and one at the end of the 8-bit intensity range. Currently, determination of the thresholds (i.e. gray lines in Fig. 1) is performed manually by the electrochemotherapy treatment planning software user. Up to five thresholds delimiting six most noticeable intensity components by clicking onto the desired targeted positions in the intensity histogram are marked.
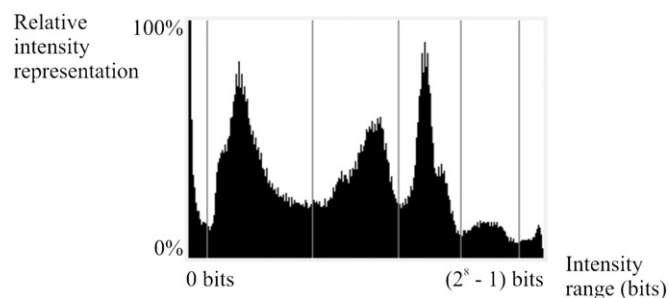

Fig. 1. An example histogram of intensities that are represented in the medical images' collection with manually determined thresholds (gray lines) between the identified main intensity components (peaks of black bars).

In the case of medical images derived from a MRI source, a contrast-enhancement procedure is applied upon the set of medical images. A basic contrast-enhancement procedure is done by performing a non-linear transformation of each pixel of each image in the collection by Eq. (1) where i denotes the *intensity* of a pixel with the range of $0 \leq i \leq 255$ and a *bit* is its unit:

$$i_N = k \cdot (i_P + 1) \cdot log_{10}(i_P + 1) \tag{1}$$

i_N is the newly calculated value by using the previous value i_P and a scaling factor k; in our case, k is empirically set to 0.5. Additionally, because of operating in the 8-bit range of intensities the newly calculated value of i_N is clamped to reside within the interval $0 \leq i_N \leq 2^8 - 1$. This procedure enhances the contrast in a non-linear way, so that distribution of intensity is changed.

Medical images may contain several unwanted artifacts (e.g. noise, gradient fill anomalies, etc.), which increases the difficulty of medical image segmentation (e.g. edges are not clearly defined) [42]. Moreover, tissue of interest to the application of electrochemotherapy (e.g. tumor, liver, brain, etc.) is most commonly heterogeneously texturized. Therefore, intensities that describe these objects (i.e. tissue) vary due to both tissue heterogeneity (low-frequency variations) and noise (high-frequency variations), making straightforward segmentation impossible (e.g. if we perform threshold-based segmentation without pre-processing, segmentation will result in many more segments than desired).

Regardless of the source of medical images, a noise removal procedure is performed by applying an average-based filter on an intensity matrix in the size of 3×3 pixels. Then, an additional noise removal is executed by applying a median-based filter on an intensity matrix in the size of 3×3 pixels that has previously already been processed using the average-based filter. Finally, the thresholds determined in the procedure of medical images' analysis (Fig. 1) are used to transform the filtered images containing continuous intensities into fully pre-processed images containing up to six discrete intensities (i.e. dithering). Dithering also takes into account heterogeneity of tissue and removes it, hence pre-processing results in homogeneous segments. The transformation is shown in Fig. 2.

As seen in Fig. 2, the pre-processing procedures may however result in non-uniform object surfaces due to source images' anomalies such as unwanted gradient fills (Fig. 2c). Nevertheless, non-uniform object surfaces do not represent a major obstacle as segmentation procedures can overcome such a limitation.

3.2.3. Segmentation

Segmentation is a complex procedure for extracting object data (i.e. usable features) from images [41], i.e. determining which part of medical images corresponds to a certain region of interest (ROI) – e.g. the liver or tumors or blood vessels. Such a procedure is performed based on the features identified in the medical images. Due to already pre-processed images, segmentation of objects from medical images is currently being done based on the intensity levels that are present in these images (i.e. threshold-based segmentation). Segments are therefore defined as clusters of pixels that all have the same intensity level [43].

To extract such segments, an algorithm termed *region growing* is applied upon the pre-processed images; the region growing algorithm is initiated by the user who manually places a starting seed on an image (i.e. clicks with the mouse somewhere on the target segment) and then the two-dimensional (i.e. based on each slice/image separately) region growing algorithm marks the desired segment on the selected image. The algorithm first checks all the eight neighboring pixels of the starting seed and if their intensities are equal to the one of the starting seed, they are indexed as being part of the target segment. The procedure is then reapplied until all the neighbors'
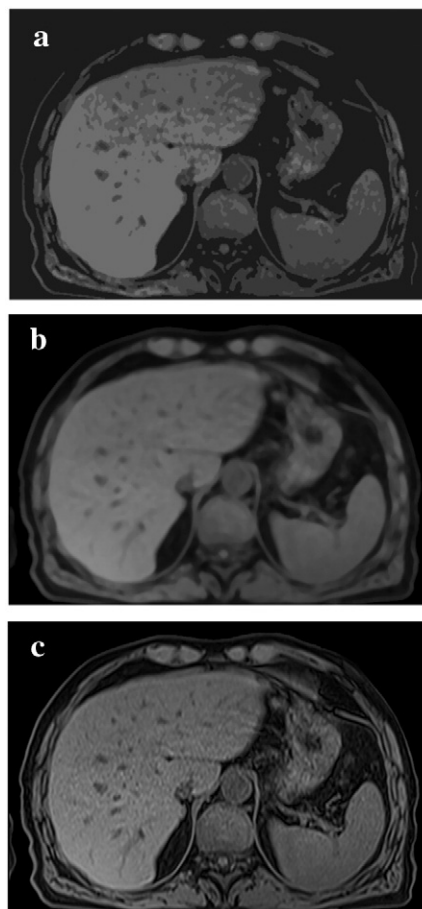

Fig. 2. An example of a CT medical image focusing on the liver; presented are a source image (left – a), a filtered image (middle – b), and a fully pre-processed image (right – c).

neighbors are indexed as well, and finished when there are no neighbors with the same intensities as the starting seed left to be indexed.

Different layers of segments can be defined (e.g. liver, vessels, tumors, etc.). Moreover, manual segmentation is possible using common drawing tools (i.e. adding or removing a single or an array of pixels to or from the selected layer), which is helpful for geometries where region growing may lead to unwanted leakage of segments.

Currently, this procedure is only performing a two-dimensional segmentation. A three-dimensional segmentation procedure is, however, planned to be implemented in the final version of the electrochemotherapy treatment planning software in order to allow more robust segmentation procedures based on three-dimensional input data since object comparison will be done on neighboring images and three-dimensional objects will be generated automatically. Moreover, more sophisticated segmentation methods than region growing shall also be considered, e.g. using deformable active contours [44].

3.2.4. Three-dimensional model generation

Before generating a three-dimensional model, segmentation data need to be appropriately post-processed in order to allow construction of a three-dimensional mesh. The post-processing algorithms evaluate all the objects that were identified in the segmentation procedure, and generate an appropriate three-dimensional mesh of the model. Evaluation of objects from the segmentation procedure is done by generating contours in a circular way by a contour-following algorithm that produces contour data as continuous sets of two-dimensional points for each medical image in the collection.

All the two-dimensional points are, finally, used as input data for the Microsoft DirectX SDK-based component that provides objects for mesh generation and visualization within the Microsoft .NET Framework v3.5 (Microsoft, Redmond, USA, 2007). To generate a three-dimensional mesh from multi-plane two-dimensional data, the *marching cubes* algorithm [45] is used. The third dimension information (i.e. step difference of the third dimension between two-dimensional segments) is obtained from the header of the source DICOM images (i.e. the slice thickness parameter).

The electrode configuration is also evaluated and implemented as a model sub-object, so that the generated mesh may be directly applicable for numerical calculations of the electric field distribution using finite-element modeling software [46].

Moreover, the generated three-dimensional model (as example shown in Fig. 3) is useful for the attending surgeon to visualize the patient's anatomy and to determine possible entry directions, which is most important in the electrode placement procedure where guidance of the attending surgeon serves as the main course of action for defining the approximate absolute position of the electrode array [47].

3.2.5. Electrode placement

Determination of the relative electrode placement depends on the size and the shape of targeted tumors. First, the number of electrodes that will be placed in the tumor needs to be determined. Namely, if the shape of the tumor that is planned for treatment is spherically asymmetrical, up to two electrodes may be planned for insertion into the tumor. In case of spherically symmetrical tumors, a single electrode may be planned for insertion into the tumor. However, even spherically symmetrical tumors may be planned for insertion of more than one electrode into the tumor if the electric field coverage could not be achieved using only one electrode being placed in the tumor due to the its size.

Then, an arbitrary number of electrodes are determined for insertion around and into the tumor. Currently, the number and the relative layout of the electrodes are limited based on the recommendations of the attending surgeon who defines possible access directions, hence the plane normal to the electrodes. Determining the number of electrodes is not strictly formalized yet, and more research needs to be performed to this end. However, the current protocol is to keep the total number of electrodes low (also to eliminate the need to manually rewire electrode-generator connections, since the currently available pulse generator has only 6 output connections), and to keep distance between adjacent electrodes below 3 cm. Fig. 4 shows an example of such a placement of the electrodes, where a single electrode was placed into the tumor and four electrodes around it.

After determining the number and the approximate relative layout of the electrodes, electrode parameters (diameter, length of the non-isolated part and the total length of the electrode) are also
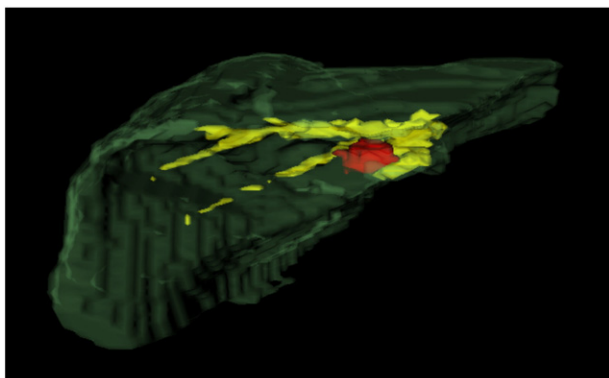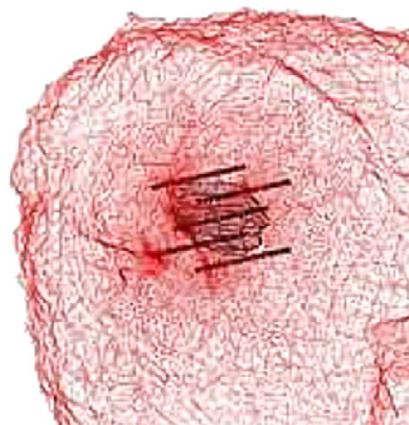

Fig. 4. An example of planned electrode placement for electrochemotherapy treatment.

defined. Finally, data of the defined electrode configuration is inserted into the three-dimensional model for electroporation modeling. The pulses are delivered to the target sequentially on pairs of electrodes, i.e. at each time only two electrodes are active. The data on the positioning and the number of electrodes need to be further supplemented by voltage amplitude of the pulses to be delivered between electrode pairs.

3.2.6. Implementation of the mathematical model of electroporation

It has been demonstrated previously that a sufficiently high local electric field is the major indicator of successful electroporation [29]. Therefore, most efforts in treatment planning and evaluation of electroporation-based treatments are currently devoted to determination of the electric field distribution in the target regions (i.e. tumor and eventually critical tissues). The electric field in conductive media is determined by solving the Laplace equation (2) for the electric potential:

$$\nabla \cdot (\sigma \cdot \nabla \varphi) = 0 \qquad (2)$$

from which the electric field can be determined by using the Eq. (3):

$$\mathbf{E} = -\nabla \cdot \varphi. \qquad (3)$$

Such a field calculation can be performed using numerical methods, e.g. the finite element [48]. We use the commercial Comsol Multiphysics (Comsol AB, Stockholm, Sweden) software, which includes a scripting interface to Matlab (Mathworks, Nantic, MA). The computational domain is split into several subdomains with different conductivities and boundary conditions (e.g. target – tumor tissue, surrounding tissues, electrodes) [33]. The outer boundaries of the computational domain are limited with an insulating boundary condition (4):

$$\mathbf{n} \cdot \mathbf{J} = 0 \qquad (4)$$

while the interior boundary conditions are defined as either continuity (5) or fixed potential (6).

$$\mathbf{n} \cdot (\mathbf{J}_1 - \mathbf{J}_2) = 0 \qquad (5)$$

$$\mathbf{V} = V_0 \qquad (6)$$

Tissue conductivities are known to change during electroporation [38]; therefore, electroporation is modeled using electric field-dependent conductivity. We used a sequential model to ensure irreversibility of conductivity changes during the duration of one pulse [26,31] while other authors use a simplified field-dependent formulation [49].

Fig. 3. A generated three-dimensional model of liver with hepatic veins and a tumor (in between the hepatic veins).

3.2.7. Algorithm-based optimization

Optimization is regularly used in radiotherapy treatment planning [50]; both gradient-based and stochastic optimization methods are commonly employed. Since the problem of optimization for electrochemotherapy involves a high number of parameters (pulse voltages, number of electrodes, position of electrodes) and therefore a very large parameter space, genetic algorithms for optimization are especially suitable [51]. The formal approach to optimization requires the formulation of an objective function, which can be a function of one or more parameters. For electrochemotherapy treatment planning, the given objective function (7) which has been proposed previously [12] can be used:

$$F = 100 \cdot V_{Trev} - 10 \cdot V_{Hirrev} \qquad (7)$$

where V_{Trev} is the volume fraction of the target tissue above the electroporation threshold (defined as the volume of tissue exposed to electric field above the tissue-specific electroporation threshold divided by the total volume of the tissue), and V_{Hirrev} is the volume fraction of the surrounding healthy tissue above the irreversible electroporation threshold. Additional terms may be added to the objective function on a case-by-case basis. The goal of the optimization is to maximize the objective function, while simultaneously ensuring that other constraints (e.g. maximum current, maximum voltage) are observed. To this end, the optimization algorithm involves changing electrode voltages, the number of electrodes and/or electrode positions. Moreover, the goal of optimization is finding a robust solution which will ensure successful treatment even in the presence of errors or unknowns in the input parameters [52].

3.3. Set-up verification

Set-up verification consists of overlaying the treatment plan, i.e. positioning of electrodes with respect to target tissue, on medical images (CT or MRI) obtained before the treatment (e.g. Fig. 5). Such an overlay in different planes is presented to the surgeon prior to the operation, the access point was determined before starting treatment planning, and then insertion of electrodes intraoperatively using ultrasound or fluoroscopy guidance is performed by the surgeon (Fig. 6a). Electrode positioning is verified by medical imaging and by measuring the depth of electrode insertion (Fig. 6b). Finally, electrodes are connected to the corresponding outputs on the pulse generator and voltages between pairs of electrodes from the treatment plan are programmed and delivered.
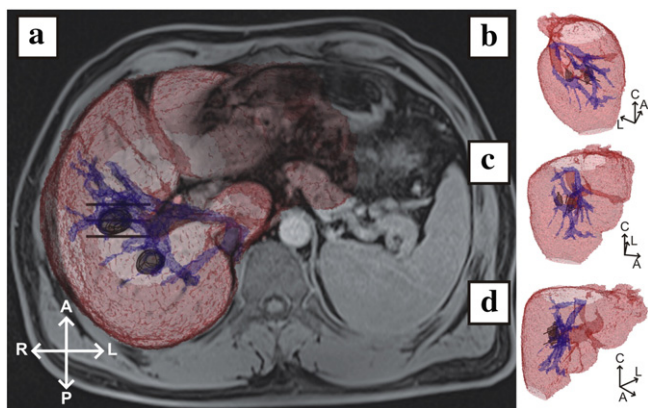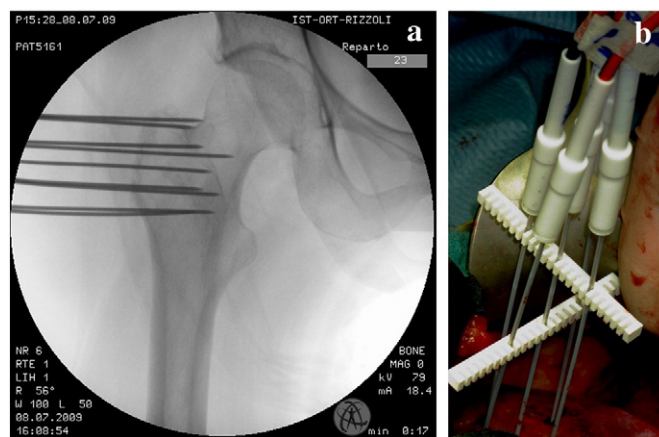

Fig. 6. a: Insertion of electrodes using fluoroscopy guidance. b: Comb-like electrode holders during electrochemotherapy surgery.

3.4. Treatment delivery and monitoring

The patient planned for electrochemotherapy is presently treated intraoperatively. The surgical team mobilizes the liver segment with the metastasis planned for treatment. The long needle electrodes (1.2 mm in diameter with 3 or 4 cm non-insulated tip – IGEA S.r.L., Carpi, MO, Italy) are inserted into the liver tissue and the tumor according to the treatment plan. The insertion of needles is image-guided and verified (as an example, Fig. 6a shows fluoroscopy guidance during bone metastasis electrochemotherapy; ultrasound guidance is used during liver electrochemotherapy). The appropriateness of needle insertion is also verified by measurement of distances between the electrodes and depth of electrode insertion, and compared to the treatment plan (Fig. 6b). Voltage and current between each pair of electrodes are measured for post processing and evaluation.

The needles are inserted using image guidance (which is needed to determine the relative position of the electrode array with respect to the target tissue) and fixed with comb-like holders (Fig. 6b), and then connected to the electric pulse generator (Cliniporator VITAE, IGEA SpA, Carpi, Italy). Thereafter the patient is given 15 000 U/m^2 of bleomycin intravenously in bolus. In the pharmacological peak, i.e. approximately 8 min after bleomycin injection, electric pulses are delivered between the electrode pairs, according to the treatment plan. The delivery of electric pulses is synchronized with the electrocardiogram (ECG); one pulse per heart-beat is delivered. This is done by the ECG triggering device, AccuSync 42 (AccuSync Medical Research Corp., Milford, CT, USA). The ECG synchronization is needed in order to avoid delivery of the electric pulse in the so-called vulnerable period of the ventricles, the T wave [53,54]. If several metastases are being treated the delivery of the electric pulses to all metastases should be performed in the time window after injection of bleomycin when tumor concentration of bleomycin is sufficiently high [55,56].

3.5. Response assessment

Response of metastases to electrochemotherapy is evaluated radiologically (CT or MRI images) and/or by histological analyses. All the patients are followed by CT or MRI imaging for possible changes in the tumor volume and/or the texture of the tumors. They are followed in a monthly period and the images are compared to the pre-treatment ones. So far, on the first 10 patients treated with electrochemotherapy no conclusive data on images were observed to predict the tumor response. Further analyses in this respect are needed. Some of the patients are on two-stage operation [27]. At the first operation, ECT is performed on some of the metastases, while the others are treated by radiofrequency ablation (RFA) or the liver segment is

Fig. 5. Overlay (a) of placed electrodes in several viewing angles (b, c, d) as a part of the treatment plan (directions: A as anterior, P as posterior, L as left, R as right, C as cranial).

ligated and scheduled for the removal at the second operation [57]. In such cases, histological analyses are possible for evaluating the histological changes in the treated lesions, especially with respect to the other, non-ECT treated metastases. Preliminary analyses indicate that ECT induces progressive degenerative changes in ECT treated metastases, indicating clinical benefit of the treatment. In some cases, even complete destruction of the treated metastasis was observed, with possible resection of the treated metastasis and no recurrence of the disease in 20 months after the treatment [15].

4. Discussion

In the last decade, electroporation-based therapies have matured, e.g. electrochemotherapy is being routinely used in the clinical setting. As electroporation-based gene therapy [5] and DNA vaccination [18,19] and ablation with irreversible electroporation are developed further [20] it is expected that in the future electroporation will become one of the commonly used clinical methods. Using electroporation for treatment of diseases of internal organs, such as deep-seated tumors, will increase the need of controlling its extent to provide more efficient treatments and minimizing the damage to the healthy tissues.

We described in some detail the development of the procedure and treatment planning software that can provide medical practitioners with the information needed to effectively use electroporation in the clinical setting. Conceptually based on radiotherapy treatment planning tools, the described protocols and algorithms have been intended specifically for electrochemotherapy of deep-seated tumors; however, they are general enough to be useful for all electroporation-based therapies given that specific details are added to the protocols and the objective function [58] is composed of the tumor tissue to be covered with a sufficiently strong electric field (above 460 V/cm, i.e. $V_{THR-rev}$) minimizing also damage to healthy tissue due to irreversible electroporation ($V_{THR-irrev}$). Voltage and electrode position/geometry with respect to the distance between electrodes need to be such as to ensure electric field strength higher than the reversible threshold ($V_{THR-rev}$) and at the same time lower than the irreversible threshold ($V_{THR-irrev}$) in order to avoid ablation of neighboring vital tissue. Similarly, a well-defined target (i.e. tumor or some other pathological tissue) needs to be determined when planning ablation using non-thermal irreversible electroporation (NTIRE). When planning an NTIRE-based treatment, the resulting electric field strength in the target tissue is required to exceed the irreversible threshold for ablation to be successful. Nevertheless, it is imperative to avoid tissue damage due to thermal effects (i.e. Joule heating) [59]. Furthermore, gene transfer for gene therapy and DNA vaccination [18,19] is another application where it is important for the resulting electric field strength in the target tissue to be above the reversible threshold and at the same time below the irreversible threshold in order to achieve sufficient gene expression [58].

All the above mentioned applications would greatly benefit from treatment planning. The procedural treatment planning software we presented is still in development and is being evaluated at the same time. However, to bring treatment planning into routine clinical use, additional considerations need to be made. First, the treatment planning software needs to be developed as an easy-to-use computer application, in order to simplify the procedure and thus to enable its widespread use. The import of medical images (CT or MRI) has to be simplified; moreover, preprocessing should be a fully automated procedure, so that the attending surgeon does not need special computer skills in order to use the software. Then, segmentation procedures for semi-automatic segmentation of medical images have to incorporate sophisticated methods that would at the same time allow easily performable segmentation (e.g. by using statistical models of organs, or by using deformable active contours). Finally, new methods of three-dimensional mesh generation need to be

established in order to adaptively generate a representative three-dimensional mesh regardless of the model being reconstructed (e.g. brain tumor, liver metastases etc.), while at the same time providing the possibility of including electrodes of arbitrary size and position.

The treatment delivery and monitoring itself also requires additional consideration. First, the treatment plan is based on the medical images (CT or MRI) of the patient that are normally acquired a few weeks before the operation; furthermore, the liver may be exposed to substantial flattening from pre-operative image scanning to intra-operative procedure [60]; moreover, during treatment delivery the liver is mobilized so that the attending surgeon can reach the targeted parts of liver for electrodes' insertion. Therefore, currently we cannot accurately match the intra-operative liver position with the generated treatment plan model as abdominal organs are deformable [61]; however, the tracking of such organs could be possible e.g. with small electromagnetically tracked sensors [47]. In the case of electroporation evolving into a percutaneous-only procedure in the future (using e.g. image guided insertion of electrodes) [62], such matching is possible. Nonetheless, in such a case the electrodes should be ultrasound-visible, which can be achieved not only by using appropriate materials (e.g. tungsten) but also by appropriately taking into consideration the scattering effect in correlation with electrodes under ultrasound [63], because materials of surgical instruments have a very high acoustic impedance [61]. Additionally, applied voltage between electrodes and the electric current should be measured during treatment delivery; in that way, conductivity measurements from real cases could be performed, and measurements' results could be re-inserted into the generated treatment plan in order to improve the algorithms used for future treatment plans (i.e. based on real feedback obtained from treatment). Visualization by Current Density Imaging (CDI) and Magnetic Resonance Electrical Impedance Tomography (MREIT) obtained during electroporation pulses might be possible in the future [64,65].

Although the described procedures for deep seated tumors electrochemotherapy based on patient-specific treatment planning rely on the radiotherapy basis, there is also a radiotherapy-specific feature that should not be replicated when planning electrochemotherapy. Namely, since in radiotherapy the damage caused by the radiation beam is not tumor-specific, it is common to plan the radiotherapy treatment to be aimed at not only target tissue (i.e. tumor), but also at a defined amount of the healthy tissue around the tumor (i.e. a safety margin); this safety margin represents a certain amount of the healthy tissue around the tumor that will be damaged by the radiation beam as well in order to assure complete beam coverage of the tumor tissue. Nevertheless, in electrochemotherapy treatment planning such increase of tumor volume is not acceptable because the tumor tissue's conductivity significantly differs from the healthy tissue's conductivity [52]. Therefore, since an exact model of the applied electric field distribution is necessary for the success of electrochemotherapy, an exact model of the patient's tissue needs to be constructed as well.

Implementation of treatment planning among the end-users (i.e. surgeons, physicians, etc.) is a challenging task. To successfully introduce treatment planning, it first needs to be validated in order to determine the accuracy and efficacy of employed procedures. The goal of this validation is to provide a known and well-controlled assessment of uncertainty, which can later be used in the numerical computation phase [47]. Validation of treatment planning is a multi-step procedure. First, segmentation needs to be validated. Validation of segmentation is possible by comparing the output of the segmentation phase to an existing database of segmented medical images; an expert opinion is then required to determine if re-segmentation of medical images using the newly developed treatment planning software matches the segments obtained from the previously available set of segmented images. Alternatively, solely expert opinion could be used to evaluate the accuracy of segmentation. Besides validation

of the segmentation, three-dimensional reconstruction needs to be validated as well. This can be done by imaging (using CT or MRI) a phantom of well-defined dimensions and shape, which is then reconstructed, and the output of the three-dimensional reconstruction is compared to the original object. Since the three-dimensional reconstruction embeds the error of segmentation, segmentation accuracy needs to be already assessed before evaluating three-dimensional reconstruction accuracy. In fact, instead of using a detailed 3D reconstruction, some studies [8] have opted for a rough approximation of the tumor and tissue geometry. While not as accurate, this simplified approach could be of great use in cases where no vital tissues are present in the electrode vicinity and can be based on approximate solutions [66–68].

Part of validation is also the follow-up procedure. To determine objective response after the treatment, the overall treatable and also measurable tumor volume needs to be determined. Pre-operative images (CT or MRI) are used to determine the overall tumor volume. Moreover, in cases of a solitary metastasis, histology should be also considered since assessment of target lesions volume shall not be the only criteria for determining objective response [69]. In our case, as part of a two stage procedure, the follow-up procedure is performed using a second surgery 4–8 weeks after the first electrochemotherapy [15]. The second surgery is necessary to extract the presumably necrotic tissue in order to perform histology and determine success of electrochemotherapy by first performing lesion measurements and then, using e.g. immunohistochemical staining, especially since etiology of necrosis can vary. Preliminary analyses indicate clinical benefit of the treatment, since in some cases even complete destruction of the treated metastasis was observed.

Additionally, several theoretical considerations have been thought of and are used in the simulations and treatment planning for electroporation-based interventions [59,70,71]. Namely, in all the described mathematical models on the tissue level electroporation is considered as a deterministic *all or nothing* response to the electric field: each cell is electroporated if exposed to electric field above electroporation threshold, and not if exposed to electric field bellow threshold. Therefore, current mathematical models of electroporation only predict electroporation based on the distribution of an applied electric field. The electric field strength is compared to a predefined threshold, and distribution is observed in the target area; if the electric field strength exceeds the predefined threshold, electroporation is predicted. However, such a model may be overly simplistic, as it overlooks the stochastic nature of electroporation [72,73]. The sources of stochasticity, for instance cell heterogeneity (e.g. in cell size, shape), cellular density and cellular communication (e.g. gap-junctions) should be included into the models [74]. In that way, more accurate treatment plans could be generated and electrochemotherapy would greatly benefit since more realistic predictions could be achieved. While the mathematical models currently used describe only the electric field distribution and changes in tissue electric properties due to electroporation, it would not be difficult to add a mathematical description of the thermal effects of the electric pulses – thermal effects can be very important for both gene electrotransfer, where due to longer pulses used more energy is deposited in the tissue, and for irreversible electroporation where it is crucial to reside below the thermal damage threshold to achieve good regeneration effects [49,75,76]. Additionally, several other mechanisms have been included in electroporation simulations, namely: mass transfer models for determining molecular uptake or transmembrane transport [77,78] and statistical methods for predicting cell death from electroporation pulses [79], all of which might be useful for specific electroporation-based therapies. Moreover, multiple treatment plans may be generated for each patient e.g. based on the genetic algorithm [80], and compared between and finally assessed with a quantitative criterion such as e.g. conformity index [81], which has already been introduced in radiotherapy.

Using numerical treatment planning protocols could ultimately lead to consistent and predictable effects, thus ensuring a maximally effective treatment. Simultaneously, treatment planning provides a framework for the development of standardized procedures as well as the ability to reduce the uncertainties inherent in the complexity of electroporation-based treatments.

Acknowledgments

References

[1] T. Kotnik, G. Pucihar, D. Miklavčič, Induced transmembrane voltage and its correlation with electroporation-mediated molecular transport, J. Membr. Biol. 236 (2010) 3–13.
[2] A. Pakhomov, D. Miklavčič, M.S. Markov, Advanced Electroporation Techniques in Biology and Medicine, CRC Press, 2010.
[3] G. Serša, D. Miklavčič, M. Čemažar, Z. Rudolf, G. Pucihar, M. Snoj, Electrochemotherapy in treatment of tumours, Eur. J. Surg. Oncol. 34 (2008) 232–240.
[4] R. Magjarević, I. Lacković, D. Miklavčič, Pet godina šire primjene elektrokemoterapije u klinici, Liječničke Novine 97 (2011) 36–39.
[5] L. Heller, R. Heller, Electroporation gene therapy preclinical and clinical trials for melanoma, Curr. Gene Ther. 10 (2010) 312–317.
[6] P. Garcia, T. Pancotto, J. Rossmeisl, N. Henao-Guerrero, N. Gustafson, G. Daniel, et al., Non-thermal irreversible electroporation (N-TIRE) and adjuvant fractionated radiotherapeutic multimodal therapy for intracranial malignant glioma in a canine patient, Technol. Cancer Res. Treat. 10 (2011) 73–83.
[7] M. Marty, G. Serša, J. Garbay, J. Gehl, C. Collins, M. Snoj, et al., Electrochemotherapy – an easy, highly effective and safe treatment of cutaneous and subcutaneous metastases: results of ESOPE (European Standard Operating Procedures of Electrochemotherapy) Study, Eur. J. Cancer Suppl. 4 (2006) 3–13.
[8] F. Mahmood, J. Gehl, Optimizing clinical performance and geometrical robustness of a new electrode device for intracranial tumor electroporation, Bioelectrochemistry 81 (2011) 10–16.
[9] B. Agerholm-Larsen, H. Iversen, P. Ibsen, J. Moller, F. Mahmood, K. Jensen, et al., Preclinical validation of electrochemotherapy as an effective treatment for brain tumors, Cancer Res. 71 (2011) 3753–3762.
[10] EU Clinical Trials Register, https://www.clinicaltrialsregister.eu/, 2011.
[11] ClinicalTrials.gov, http://clinicaltrials.gov/, 2011.
[12] D. Miklavčič, M. Snoj, A. Županič, B. Kos, M. Čemažar, M. Kropivnik, et al., Towards treatment planning and treatment of deep-seated solid tumors by electrochemotherapy, Biomed. Eng. Online 9 (2010).
[13] M. Fini, M. Tschon, M. Alberghini, G. Bianchi, M. Mercuri, L. Campanacci, et al., Cell Electroporation in Bone Tissue, in: S.T. Kee, J. Gehl, E.W. Lee (Eds.), Clinical Aspects of Electroporation, Springer New York, New York, NY, 2011.
[14] J. Rossmeisl, P. Garcia, O. Lanz, N. Henao-Guerrero, R. Davalos, Successful treatment of a large soft tissue sarcoma with irreversible electroporation, J. Clin. Oncol. 29 (2011) E372–E377.
[15] I. Edhemović, E.M. Gadžijev, E. Brecelj, D. Miklavčič, B. Kos, A. Županič, et al., Electrochemotherapy: a new technological approach in treatment of metastases in the liver, Technol. Cancer Res. Treat. 10 (2011) 475–485.
[16] M. Kandušer, D. Miklavčič, M. Pavlin, Mechanisms involved in gene electrotransfer using high- and low-voltage pulses – an in vitro study, Bioelectrochemistry 74 (2009) 265–271.
[17] F. Andre, J. Gehl, G. Serša, V. Preat, P. Hojman, J. Eriksen, et al., Efficiency of high and low voltage pulse combinations for gene electrotransfer in muscle, liver, tumor and skin, Hum. Gene Ther. 19 (2008) 1261–1271.
[18] J.J. Kim, Electroporation-enhanced delivery of DNA vaccines, Bioprocess Int. 9 (2011) 10–14.
[19] N.Y. Sardesai, D.B. Weiner, Electroporation delivery of DNA vaccines: prospects for success, Curr. Opin. Immunol. 23 (2011) 421–429.
[20] P.A. Garcia, J.H. Rossmeisl, R.E. Neal, T.L. Ellis, J.D. Olson, N. Henao-Guerrero, et al., Intracranial nonthermal irreversible electroporation: in vivo analysis, J. Membr. Biol. 236 (2010) 127–136.
[21] G. Onik, B. Rubinsky, Irreversible Electroporation: First Patient Experience Focal Therapy of Prostate Cancer, in: B. Rubinsky (Ed.), Irreversible Electroporation, Springer-Verlag, Berlin Heidelberg, 2010, pp. 235–247.
[22] K.P. Charpentier, F. Wolf, L. Noble, B. Winn, M. Resnick, D.E. Dupuy, Irreversible electroporation of the pancreas in swine: a pilot study, HPB. 12 (2010) 348–351.
[23] M. Lecchi, P. Fossati, F. Elisei, R. Orecchia, G. Lucignani, Current concepts on imaging in radiotherapy, Eur. J. Nucl. Med. Mol. Imaging 35 (2008) 821–837.
[24] I.F. Tannock, R.P. Hill, R.G. Bristow, L. Harrington, The Basic Science of Oncology, 4th ed. McGraw-Hill Medical, 2005.
[25] D.E. Lea, The mechanisms of the induction by radiation of chromosome aberrations in Tradescantia, J. Genet. 44 (1942) 216–245.

[26] D. Šel, D. Cukjati, D. Batiuskaite, T. Slivnik, L. Mir, D. Miklavčič, Sequential finite element model of tissue electropermeabilization, IEEE Trans. Biomed. Eng. 52 (2005) 816–827.
[27] H.D. González, J. Figueras, Practical questions in liver metastases of colorectal cancer: general principles of treatment, HPB. 9 (2007) 251–258.
[28] D. Šemrov, D. Miklavčič, Calculation of the electrical parameters in electrochemotherapy of solid tumours in mice, Comput. Biol. Med. 28 (1998) 439–448.
[29] D. Miklavčič, K. Beravs, D. Šemrov, M. Čemažar, F. Demšar, G. Serša, The importance of electric field distribution for effective in vivo electroporation of tissues, Biophys. J. 74 (1998) 2152–2158.
[30] D. Šemrov, D. Miklavčič, Numerical modeling for in vivo electroporation, Methods Mol. Med. 37 (2000) 63–81.
[31] D. Miklavčič, D. Šemrov, H. Mekid, L. Mir, A validated model of in vivo electric field distribution in tissues for electrochemotherapy and for DNA electrotransfer for gene therapy, Biochim. Biophys. Acta Gen. Subj. 1523 (2000) 73–83.
[32] S. Čorović, A. Županič, S. Kranjc, B. Al Sakere, A. Leroy-Willig, L. Mir, et al., The influence of skeletal muscle anisotropy on electroporation: in vivo study and numerical modeling, Med. Biol. Eng. Comput. 48 (2010) 637–648.
[33] N. Pavšelj, Z. Bregar, D. Cukjati, D. Batiuskaite, L. Mir, D. Miklavčič, The course of tissue permeabilization studied on a mathematical model of a subcutaneous tumor in small animals, IEEE Trans. Biomed. Eng. 52 (2005) 1373–1381.
[34] P. Canatella, J. Karr, J. Petros, M. Prausnitz, Quantitative study of electroporation-mediated molecular uptake and cell viability, Biophys. J. 80 (2001) 755–764.
[35] G. Pucihar, J. Krmelj, M. Reberšek, T. Batista-Napotnik, D. Miklavčič, Equivalent pulse parameters for electroporation, IEEE Trans. Biomed. Eng. 58 (2011) 3279–3288.
[36] H. He, D.C. Chang, Y.-K. Lee, Using a micro electroporation chip to determine the optimal physical parameters in the uptake of biomolecules in HeLa cells, Bioelectrochemistry 70 (2007) 363–368.
[37] M. Pavlin, M. Kandušer, M. Reberšek, G. Pucihar, F. Hart, R. Magjarević, et al., Effect of cell electroporation on the conductivity of a cell suspension, Biophys. J. 88 (2005) 4378–4390.
[38] D. Cukjati, D. Batiuskaite, F. Andre, D. Miklavčič, L. Mir, Real time electroporation control for accurate and safe in vivo non-viral gene therapy, Bioelectrochemistry 70 (2007) 501–507.
[39] E. Maor, A. Ivorra, B. Rubinsky, Non thermal irreversible electroporation: novel technology for vascular smooth muscle cells ablation, PLoS One 4 (2009) E4757.
[40] Medical Imaging & Technology Alliance (a division of NEMA), Digital Imaging and Communications in Medicine – DICOM, http://medical.nema.org/2011.
[41] S. Ahmed, K. Iftekharuddin, A. Vossough, Efficacy of texture, shape, and intensity feature fusion for posterior-fossa tumor segmentation in MRI, IEEE Trans. Inf. Technol. Biomed. 15 (2011) 206–213.
[42] Z. Ma, J. Tavares, R. Jorge, T. Mascarenhas, A review of algorithms for medical image segmentation and their applications to the female pelvic cavity, Comput. Methods Programs Biomed. 13 (2010) 235–246.
[43] M. Mancas, B. Gosselin, B. Macq, Segmentation Using a Region Growing Thresholding, in: Image Processing: Algorithms and Systems IV, Image Processing: Algorithms and Systems IV, San Jose, CA, USA, 2005.
[44] C. Xu, J.L. Prince, Snakes, shapes, and gradient vector flow, IEEE Trans. Image Process. 7 (1998) 359–369.
[45] W.E. Lorensen, H.E. Cline, Marching cubes: a high resolution 3D surface construction algorithm, ACM Comput. Graph. 21 (1987) 163–169.
[46] D. Pahr, P. Zysset, From high-resolution CT data to finite element models: development of an integrated modular framework, Comput. Methods Biomech. Biomed. Engin. 12 (2009) 45–57.
[47] K. Cleary, T. Peters, Image-guided interventions: technology review and clinical applications, Annu. Rev. Biomed. Eng. 12 (2010) 119–142.
[48] N. Pavšelj, D. Miklavčič, Numerical modeling in electroporation-based biomedical applications, Radiol. Oncol. 42 (2008) 159–168.
[49] P. Garcia, J. Rossmeisl, R. Neal, T. Ellis, R. Davalos, A parametric study delineating irreversible electroporation from thermal damage based on a minimally invasive intracranial procedure, Biomed. Eng. Online 10 (2011) 34.
[50] V. Bevilacqua, G. Mastronardi, G. Piscopo, Evolutionary approach to inverse planning in coplanar radiotherapy, Image Vis. Comput. 25 (2007) 196–203.
[51] J.H. Holland, Adaptation in Natural and Artificial Systems: An Introductory Analysis with Applications to Biology, Control, and Artificial Intelligence, A Bradford Book, 1992.
[52] B. Kos, A. Županič, T. Kotnik, M. Snoj, G. Serša, D. Miklavčič, Robustness of treatment planning for electrochemotherapy of deep-seated tumors, J. Membr. Biol. 236 (2010) 147–153.
[53] A. Deodhar, T. Dickfeld, G. Single, W. Hamilton, R. Thornton, C. Sofocleous, et al., Irreversible electroporation near the heart: ventricular arrhythmias can be prevented with ECG synchronization, Am. J. Roentgenol. 196 (2011) W330–W335.

[54] B. Mali, T. Jarm, S. Čorović, M. Paulin-Košir, M. Čemažar, G. Serša, et al., The effect of electroporation pulses on functioning of the heart, Med. Biol. Eng. Comput. 46 (2008) 745–757.
[55] L. Mir, J. Gehl, G. Sersa, C. Collins, J. Garbay, V. Billard, et al., Standard operating procedures of the electrochemotherapy: instructions for the use of bleomycin or cisplatin administered either systemically or locally and electric pulses delivered by the Cliniporator (TM) by means of invasive or non-invasive electrodes, Eur. J. Cancer Suppl. 4 (2006) 14–25.
[56] R.T. Dorr, Bleomycin pharmacology: mechanism of action and resistance, and clinical pharmacokinetics, Semin. Oncol. 19 (1992) 3–8.
[57] R. Finch, H. Malik, Z. Hamady, A. Al-Mukhtar, R. Adair, K. Prasad, et al., Effect of type of resection on outcome of hepatic resection for colorectal metastases, Br. J. Surg. 94 (2007) 1242–1248.
[58] A. Županič, S. Čorović, D. Miklavčič, M. Pavlin, Numerical optimization of gene electrotransfer into muscle tissue, Biomed. Eng. Online 9 (2010) 66.
[59] A. Županič, D. Miklavčič, Tissue heating during tumor ablation with irreversible electroporation, Electrotech. Rev. 78 (2011) 42–47.
[60] L.W. Clements, P. Dumpuri, W.C. Chapman, B.M. Dawant, R.L. Galloway, M.I. Miga, Organ surface deformation measurement and analysis in open hepatic surgery: method and preliminary results from 12 clinical cases, IEEE Trans. Biomed. Eng. 58 (2011) 2280–2289.
[61] D. Hawkes, D. Barratt, J. Blackall, C. Chan, P. Edwards, K. Rhode, et al., Tissue deformation and shape models in image-guided interventions: a discussion paper, Med. Image Anal. 9 (2005) 163–175.
[62] S. Phee, K. Yang, Interventional navigation systems for treatment of unresectable liver tumor, Med. Biol. Eng. Comput. 48 (2010) 103–111.
[63] J.M. Mari, C. Cachard, Ultrasonic scanning of straight micro tools in soft biological tissues: methodology and implementation, Ultrasonics 51 (2011) 632–638.
[64] M. Kranjc, F. Bajd, I. Serša, D. Miklavčič, Magnetic resonance electrical impedance tomography for monitoring electric field distribution during tissue electroporation, IEEE Trans. Med. Imaging 30 (2011) 1771–1778.
[65] I. Serša, Enhanced sensitivity current density imaging, J. Magn. Reson. 204 (2010) 219–224.
[66] S. Čorović, M. Pavlin, D. Miklavčič, Analytical and numerical quantification and comparison of the local electric field in the tissue for different electrode configurations, Biomed. Eng. Online 6 (2007).
[67] R. Jimenez, A. Pupo, J. Cabrales, J. Joa, L. Cabrales, J. Nava, et al., 3D stationary electric current density in a spherical tumor treated with low direct current: an analytical solution, Bioelectromagnetics 32 (2011) 120–130.
[68] S. Dev, D. Dhar, W. Krassowska, Electric field of a six-needle array electrode used in drug and DNA delivery in vivo: analytical versus numerical solution, IEEE Trans. Biomed. Eng. 50 (2003) 1296–1300.
[69] M. Fabel, H. Bolte, H. von Tengg-Kobligk, L. Bornemann, V. Dicken, S. Delorme, et al., Semi-automated volumetric analysis of lymph node metastases during follow-up-initial results, Eur. Radiol. 21 (2011) 683–692.
[70] R. Davalos, B. Rubinsky, Temperature considerations during irreversible electroporation, Int. J. Heat Mass Transf. 51 (2008) 5617–5622.
[71] R. Davalos, B. Rubinsky, L. Mir, Theoretical analysis of the thermal effects during in vivo tissue electroporation, Bioelectrochemistry 61 (2003) 99–107.
[72] B. Henslee, A. Morss, X. Hu, G. Lafyatis, L. Lee, Electroporation dependence on cell size: optical tweezers study, Anal. Chem. 83 (2011) 3998–4003.
[73] M. Puc, T. Kotnik, L. Mir, D. Miklavčič, Quantitative model of small molecules uptake after in vitro cell electropermeabilization, Bioelectrochemistry 60 (2003) 1–10.
[74] L. Towhidi, T. Kotnik, G. Pucihar, S. Firoozabadi, H. Mozdarani, D. Miklavčič, Variability of the minimal transmembrane voltage resulting in detectable membrane electroporation, Electromagn. Biol. Med. 27 (2008) 372–385.
[75] I. Lacković, R. Magjarević, D. Miklavčič, Three-dimensional finite-element analysis of joule heating in electrochemotherapy and in vivo gene electrotransfer, IEEE Trans. Dielectr. Electr. Insul. 16 (2009) 1338–1347.
[76] N. Pavšelj, D. Miklavčič, Resistive heating and electropermeabilization of skin tissue during in vivo electroporation: a coupled nonlinear finite element model, Int. J. Heat Mass Transf. 54 (2011) 2294–2302.
[77] Y. Granot, B. Rubinsky, Mass transfer model for drug delivery in tissue cells with reversible electroporation, Int. J. Heat Mass Transf. 51 (2008) 5610–5616.
[78] D. Miklavčič, L. Towhidi, Numerical study of the electroporation pulse shape effect on molecular uptake of biological cells, Radiol. Oncol. 44 (2010) 34–41.
[79] A. Goldberg, B. Rubinsky, The effect of electroporation type pulsed electric fields on DNA in aqueous solution, Technol. Cancer Res. Treat. 9 (2010) 423–430.
[80] A. Županič, D. Miklavčič, Optimization and Numerical Modeling in Irreversible Electroporation Treatment Planning, in: Irreversible Electroporation, Springer, Berlin, 2009, pp. 203–222.
[81] L. Feuvret, G. Noel, J. Mazeron, P. Bey, Conformity index: A review, Int. J. Radiat. Oncol. 64 (2006) 333–342.